

# Notes for PHYS 233: Interstellar Medium

Bill Wolf

February 21, 2014

# Contents

<b>1</b>	<b>Introduction</b>	<b>4</b>
1.1	Organization of the ISM in the Milky Way . . . . .	4
1.1.1	Gas Content . . . . .	4
1.1.2	Energy Content . . . . .	6
1.1.3	Galactic Endgame . . . . .	6
1.2	Basics of Diffuse Gas . . . . .	6
<b>2</b>	<b>Collisionally Excited Lines</b>	<b>7</b>
2.1	Two-Level Atom . . . . .	8
2.2	Three-Level Atom . . . . .	10
2.3	Energy Level Diagrams . . . . .	12
2.4	Infrared Line Diagnostics . . . . .	13
2.5	Resonance Lines and Selection Rules . . . . .	13
2.5.1	Hydrogen Line Series . . . . .	14
<b>3</b>	<b>Molecular Spectra</b>	<b>14</b>
3.1	Rotating Molecules . . . . .	14
3.2	Vibrating Molecules . . . . .	14
3.3	Molecular Hydrogen . . . . .	14
<b>4</b>	<b>Transition Rates</b>	<b>15</b>
<b>5</b>	<b>Radiative Transfer</b>	<b>15</b>
5.1	Basic Definitions . . . . .	16
5.2	Equation of Radiative Transfer . . . . .	17
5.2.1	Example: Lyman Alpha Forest from AGNs . . . . .	17
5.2.2	Optical Depth . . . . .	18
5.2.3	Radio Astronomy . . . . .	19
5.3	Resonance Line Transfer . . . . .	19
5.3.1	The Voigt Profile . . . . .	19
5.3.2	21 cm Line . . . . .	22
<b>6</b>	<b>Additional Microphysics</b>	<b>23</b>
6.1	Emission and Absorption by a Thermal Plasma . . . . .	23
6.2	Collisional Ionization Equilibrium . . . . .	25
<b>7</b>	<b>H II Regions</b>	<b>25</b>
7.1	Thermal Equilibrium . . . . .	25
7.1.1	Photoionization Heating . . . . .	25
7.1.2	Cooling By Recombination . . . . .	26
7.1.3	Collisional Cooling . . . . .	27
7.2	Strömgren Spheres . . . . .	28
7.2.1	Ionization Equilibrium of a Pure H Nebula . . . . .	28
7.2.2	The Strömgren Radius . . . . .	29
7.2.3	Ionization Parameter . . . . .	30

---

7.2.4	Effects of Helium . . . . .	31
<b>8</b>	<b>Dust</b>	<b>32</b>
8.1	Evidence for Dust Grains . . . . .	32
8.2	Obscuring Effects of Dust . . . . .	33
8.3	Thermal Properties of Grains . . . . .	34

# 1 Introduction

*Monday, January 6, 2013*

This course is called “Interstellar Medium” (ISM), but really it is about the more general topic of the physics of diffuse gas in the universe. By diffuse, we mean *really* diffuse, down to number densities of  $1\text{ cm}^{-3}$ , much more diffuse than the best vacuums in terrestrial laboratories. This includes the interstellar gas in galaxies as well as the intergalactic gas in between the galaxies.

## 1.1 Organization of the ISM in the Milky Way

Interstellar gas is what forms the stars in galaxies that are the dominant sources of energy and light in the universe. Thus, understanding the physics of the ISM helps us understand (and predict) the visible appearance of galaxies.

The space between the stars is occupied by gas, dust, cosmic rays, electromagnetic radiation (from stars, the CMB, and radiation from interstellar matter), neutrinos, dark matter particles (whatever they are), and magnetic and gravitational fields. Do note that dust is distinct from gas, as dust grains have a lengthscale (micron) four orders of magnitude greater than gas particles (angstrom).

In the Milky Way, there is roughly  $10^{11} M_{\odot}$  in various components:

- $5 \times 10^{10} M_{\odot}$  of stars
- $5 \times 10^{10} M_{\odot}$  of dark matter
- $7 \times 10^9 M_{\odot}$  of interstellar gas

So the Milky Way is a rather gas-poor galaxy. Other galaxies like the Magellanic clouds have most of their baryons in the gas phase. The obscuration in the central disk of the Milky Way is produced by the dust along the midplane (see color plate in 1.2, 1.65, 2.2  $\mu\text{m}$  images). While the stars do form in a very thin disk (thin compared to its width), the starlight heats up dust and expands the dust disk to higher altitudes from the midplane.

The magnetic fields in the Milky Way can be detected by looking for synchrotron emission (caused by electrons spiraling around galactic field lines). We do observe this emission (see additional plate) and believe the magnetic fields are caused by a dynamo effect due to the circulating galactic material.

### 1.1.1 Gas Content

There is about  $5 \times 10^9 M_{\odot}$  of hydrogen in the Milky Way, in the following states

- $2.9 \times 10^9 M_{\odot}$  of H I gas (neutral)
- $1.12 \times 10^9 M_{\odot}$  of H II gas (ionized)
- $0.84 \times 10^9 M_{\odot}$  of  $\text{H}_2$  gas (molecular)

We can track the presence of interstellar gas by looking at  $C^+$  emission in the Milky Way, which tracks hydrogen presence very well, though the weighting is different since the emission strength is proportional to the density squared.

Finally, we track galactic gas via CO emission, which is very concentrated to the disk, but also has strong filaments outside the central disk of the galaxy.

The interstellar medium exhibits turbulence that is the result of supernovae and other violent hydrodynamic events.

**Phases of Interstellar Gas** We categorize the ISM into various phases according to the ionization/molecular state of its hydrogen (descriptions taken from Draine 1.1):

- **Warm H I** : Neutral hydrogen gas at temperatures around  $T \approx 10^{3.7}$  K. Typically at densities of  $n_H \approx 0.6 \text{ cm}^{-3}$ . Occupies about 40% of the galactic disk. Often referred to as the warm neutral medium (WNM)
- **Cool H I** : Neutral hydrogen gas at temperatures around  $T \approx 100$  K with higher densities of  $n_H \approx 30 \text{ cm}^{-3}$ . Occupies around 1% of the local ISM, sometimes referred to as the cold neutral medium (CNM)
- **Diffuse H<sub>2</sub>**: Like the CNM, but with larger densities and column densities, allowing molecular hydrogen ( $H_2$ ) to be more abundant.
- **Dense H<sub>2</sub>**: Gravitationally bound clouds with number densities exceeding  $10^3 \text{ cm}^{-3}$ . Distinguished by their dark appearance (strong optical extinction) in their central regions. Hosts of star formation. Not “dense” by terrestrial standards.
- **Ionized H II** at  $10^4$  K: Gas consisting largely of photoionized hydrogen, likely from ultraviolet radiation from a nearby massive star. May be dense material from a cloud (H II region) or diffuse intercloud material (diffuse H II). Lifetimes typically on the order of that of a massive star (Myrs). Extended diffuse photoionized regions, sometimes called the warm ionized medium (WIM), contain *much* more total mass than the more visible H II regions. Planetary nebulae (PNe) are also in this class.
- **Coronal Gas** (Ionized H II at  $\log T > 5.5$ ): Very hot, ionized gas that has been shock-heated by blastwaves from supernova explosions. It is mostly collisionally ionized with some exotic ionization states present. Typically very low density, filling about half the volume of the galactic disk. Cools on Myr timescales. Often referred to as the hot ionized medium (HIM).

**Elemental Composition** The gas is largely made of hydrogen and helium from the early universe, but an additional 1-2% (by mass) is heavy elements ( $Z > 2$ ), or to astronomers, “metals”. The metallicity is actually a declining function from the center of the galaxy outwards since it is the result of stellar processing, and the center of the galaxy is more evolved than its relatively young outer regions. The metallicity near the solar system is about half of that at the galactic center. We know the local composition of the ISM by measuring solar photospheric abundances and the composition of meteorites (See table 1.4 in Draine).

Energy Type	Density ( $\text{eV cm}^{-3}$ )
Thermal	0.49
Bulk Kinetic	0.22
Cosmic Ray	1.39
Magnetic	0.89
CMB	0.265
Far infrared from dust	0.31
Starlight	0.54

Table 1: Energy densities in the ISM.

### 1.1.2 Energy Content

Energy in the CMB has a strange equipartition where nearly all components are near  $1 \text{ eV cm}^{-3}$ . Some of this is self-sustaining, but since the CMB energy density increases as  $(1+z)^4$ , its equality is coincidental. The rough energy densities by categories are given in Table 1. Since the galactic magnetic fields are driven by bulk motions, it is unsurprising that the turbulent (bulk) and magnetic energies are nearly equal. If the cosmic ray energy density were significantly greater, the magnetic fields could not confine them, so they would simply escape the galaxy. Similarly, if the energy from starlight were significantly higher, the ISM would expand and likely dampen star formation, causing the near equipartition that we observe. If any of these components grows much larger than the gravitational binding energy, then hydrostatic equilibrium is disrupted, driving a wind. All galaxies drive winds at some time.

### 1.1.3 Galactic Endgame

All of the ISM constituents are present between galaxies, and the same physical processes apply to studying the intergalactic medium (IGM). In our present state of the field, we can't account for the relative overabundance of dark matter in the vicinity of a galaxy. It is thought that the “missing baryons” are in the circum-galactic material (CGM). The only place where the mass is “right” is in massive clusters. What is unknown is what sort of lengthscale determines how far out this CGM might extend. Interestingly, the material observed in the CGM contains metals, so either galactic winds are responsible for pushing material processed by stellar evolution out of the galaxy, or very massive population III stars formed at  $z \sim 20 - 40$  to form the first metals.

## 1.2 Basics of Diffuse Gas

Perhaps the prettiest regions of diffuse gas are the H II regions, like the Orion Nebula, which is illuminated by four central stars (the trapezium). The typical H II region has a number density around  $1 \text{ cm}^{-3}$  and a temperature of  $10^4 \text{ K}$ . A big difference between these H II regions (and in fact most instances of interstellar gas) and stellar interiors is that they are *not* in local thermodynamic equilibrium (LTE).

The NLTE-ness of diffuse gas is due to the much, much lower collision rate than in planetary atmospheres or stellar interiors. In order to achieve LTE, a gas must satisfy the following conditions:

Environment	Number Density ( $\text{cm}^{-3}$ )	Collision Timescale (s)
Earth Atmosphere	$2 \times 10^{13}$	$\sim 10^{-9}$
Molecular Cloud	$10^6$	$10^8$ (several days)
ISM	1	$10^{11}$ ( $10^4$ yr)

Table 2: Some characteristic collision timescales.

- Population of excited states given by Boltzmann equilibrium
- Particle energies distributed according to the Maxwell distribution
- Ionization balance given by Saha Equation
- Photon energies described by Planck Function

In diffuse gas, we may indeed be able to identify a kinetic temperature that gives the average kinetic energy of the particles, but this temperature need not be the same as the Boltzmann temperature, which gives the occupation of energy states in the system. Likewise, the ionization temperature, Planck temperature (of a blackbody), and other such derived temperatures need not match such a diffuse system.

## 2 Collisionally Excited Lines

*Wednesday, January 8, 2014*

A typical timescale for collisions between particles can be estimated via

$$\tau = \frac{1}{\sigma v n} \quad (2.1)$$

That is, it's essentially the inverse of the expected collision rate. Here  $\sigma$  is the cross section for interaction,  $v$  is the relative velocity of particles, and  $n$  is the number density of particles. Some typical timescale for various environments are given in Table 2.

Also of importance is the volumetric rate of emission of photons due to recombination, which will be proportional to the product of electron and ion number densities, or  $r_{\text{emis}} \propto n_{\text{ion}} n_e$ . We define the **Emission Measure** as

$$\text{EM} = \int n_e^2 ds \quad (2.2)$$

where the integral is over some path in space. The “natural” units for this measure is then  $\text{pc cm}^{-6}$ .

**Example: Emission Measure of a Nova Shell** For a nova shell with mass  $\Delta M = 10^{-4} M_{\odot}$  expanding with a velocity  $v = 10^3 \text{ km s}^{-1}$ , we get an approximate emission measure of

$$\text{EM} = (3 \times 10^{-4} \text{ pc})(10^7 \text{ cm}^{-3}) \sim 3 \times 10^{10} \text{ pc cm}^{-6} \quad (2.3)$$

So at early times nova shells are very bright. We could play this game with other objects like planetary nebulae (PNe), H II Regions, Diffuse warm-ionized gas, or circumgalactic gas to get an idea of how bright these objects would appear.

## 2.1 Two-Level Atom

If we consider an atom that has only two states, 1 and 2, with degeneracies  $g_1$  and  $g_2$  with an energy gap  $\epsilon_{12}$ , the collisional cross section is given by

$$\sigma_{12}(E) = \frac{h^2}{8\pi m_e E} \frac{\Omega_{12}(E)}{g_1} \quad (2.4)$$

where  $\Omega$  is the **collision strength**, which is a dimensionless quantity with values around order unity. The **Principle of Detailed Balance**, which we have not yet proven, tells us that  $\Omega_{12} = \Omega_{21}$ .

Indeed, the principle of detailed balance tells us that the rate of upwards and downward collisional transitions are equal, or

$$R_{12} = R_{21} \quad (2.5)$$

$$n_1 n_e \alpha_{12} = n_2 n_e \alpha_{21} \quad (2.6)$$

where  $\alpha$  is the collisional excitation coefficient for that reaction. To derive this principle, we turn to statistical mechanics, and the concept of a **partition function**, which is the normalization to a boltzmann distribution:

$$Z(T) \equiv \sum_s e^{-E(s)/(kT)} \quad (2.7)$$

where the sum is over all microstates. In a dilute gas, the partition function is actually a product of the partition functions from the internal system and that of the translational system:

$$Z(T) = Z_{\text{trans}}(T) \times Z_{\text{int}}(T) \quad (2.8)$$

Then we can define the partition function per unit volume in the usual way

$$f(T) = \frac{Z(T)}{V} \quad (2.9)$$

$$= \left( \frac{2\pi M_x kT}{h^3} \right)^{3/2} \times Z_{\text{int}}(T) \quad (2.10)$$

Where we've glossed over some details present in Draine (Chapter 3). Using statistical mechanics, we are more or less assuming we are in LTE, so the number densities of various states for the reaction



is given in the usual way:

$$\frac{n_{\text{LTE}}(C)}{n_{\text{LTE}}(A)n_{\text{LTE}}(B)} = \frac{f(C)}{f(A)f(B)} \quad (2.12)$$



which constrains the rate coefficients in a specific way. Armed with this tool, we can actually try to compute collisional excitation rates:

$$R_{12} = n_1 n_e \int_{E_{12}}^{\infty} \sigma(v) v f(v) dv \quad (2.13)$$

$$R_{21} = n_2 n_e \int_0^{\infty} \sigma(v) v f(v) dv \quad (2.14)$$

Now using the principle of detailed balance, we equate these rates and get

$$n_1 e^{-E_{12}/(kT)} \frac{\Omega_{12}}{g_1} = \frac{n_2 \Omega_{21}}{g_2} \quad (2.15)$$

Solving for the ratio of the number densities, we get

$$\frac{n_2}{n_1} = \frac{\alpha_{12}}{\alpha_{21}} = \frac{\Omega_{21}}{g_1} \frac{g_2}{\Omega_{12}} e^{-E_{12}/(kT)} \quad (2.16)$$

Or, more simply

$$\frac{n_2}{n_1} = \frac{\Omega_{21}}{\Omega_{12}} \frac{g_2}{g_1} e^{-E_{12}/(kT)} \quad (2.17)$$

Now if we are in LTE, we immediately recover  $\Omega_{21} = \Omega_{12}$  since the Boltzmann ratio is already present. However, the collision strength is an intrinsic property of the ion, so this must be true in all cases. That is, we don't require LTE to recover  $\Omega_{12} = \Omega_{21}$  simply because we proved that it *does* apply in LTE, and thus at all times.

In the low density limit, spontaneous decay dominates emission since collisionally excited transitions are few and far between. Then the transition rate can be written as

$$n_e n_1 \alpha_{12} = n_2 A_{21} \quad (2.18)$$

where  $A$  is the **Einstein Coefficient** for spontaneous decay from state 2 to state 1.

$$F_{12} = E_{12} A_{21} n_2 \quad (2.19)$$

Subbing in some Boltzmann algebra,  $n_2$  can be expressed as

$$n_2 = \frac{n_e n_1}{A_{21}} \left( \frac{2\pi\hbar^4}{km_e^3} \right)^{1/2} \frac{\Omega_{12}}{g_1} \frac{e^{-E_{12}/(kT)}}{\sqrt{T}} \quad (2.20)$$

Plugging (2.20) into (2.19) and evaluating some of the constants, we get

$$F_{12} = E_{21} n_e n_1 (8.62942 \times 10^{-6}) \frac{1}{\sqrt{T}} \frac{\Omega_{12}}{g_1} e^{-E_{12}/(kT)} \quad (2.21)$$

Now in the high density limit, we do something similar, getting

$$n_e n_1 \alpha_{12} = n_2 A_{21} + n_e n_2 \alpha_{21} \quad (2.22)$$

Now we get

$$F_{12} = E_{21} A_{21} n_1 \frac{g_2}{g_1} e^{-E_{12}/(kT)} \quad (2.23)$$

These two regimes beg for us to define a critical density that separates these two limits where  $n_2 A_{21} = n_2 n_e \alpha_{21}$ , which is, after some algebra,

$$n_{e,\text{crit}} = \frac{A_{21} g_2 T^{1/2}}{\beta \Omega_{12}} \quad (2.24)$$

where

$$\beta \equiv \left[ \frac{2\pi \hbar^4}{k m_e^3} \right]^{1/2} \quad (2.25)$$

For forbidden lines, this critical density is in the range of  $10^2 - 10^7 \text{ cm}^{-3}$ . For intercombination lines, the critical density is around  $10^{10} \text{ cm}^{-3}$ . For resonance lines (aka permitted lines), the critical density is  $10^{15} \text{ cm}^{-3}$

## 2.2 Three-Level Atom

*Friday, January 10, 2014*

### Suggested References

- Dopita & Sutherland Chapter 3

Now we consider the slightly more complicated three-level atom. Considering that the collisional excitation rate is, in general, given by

$$C_{ij} = n_e \alpha_{ij} \quad (2.26)$$

for the appropriate rate factors  $\alpha_{ij}$  for excitations from state  $i$  to state  $j$ . Now we'll employ statistical equilibrium to figure out the equilibrium rates and concentrations. For level 3, we get the following

$$n_1 C_{13} + n_2 C_{23} = n_3 (C_{31} + C_{32} + A_{32} + A_{31}) \quad (2.27)$$

now for level 2, we get

$$n_1 C_{12} + n_3 (C_{32} + A_{32}) = n_2 (C_{21} + C_{23} + A_{21}) \quad (2.28)$$

and for normalization purposes, let's assume that the total number density is given by  $n$ :

$$n_1 + n_2 + n_3 = n \quad (2.29)$$

(2.27) and (2.28) essentially just equate the rates of reactions (collisional or spontaneous) for the "formation" of that energy state (left side) to the rates of "destruction" rates (right side).

Now we'll make some assumptions, namely that the energy levels are roughly equally spaced, or  $E_{12} \approx E_{23}$ . This tells us that the rate of excitations from state 1 to state 3 will be much lower than

that from state 1 to state 2, or  $C_{13} \gg C_{12}$ . Now in a low density limit, we may ignore collisional excitation, which reduces our equations to a much cleaner form:

$$n_1 C_{13} = n_3 (A_{32} + A_{31}) \quad (2.30)$$

$$n_1 C_{12} + n_3 A_{32} = n_2 A_{21} \quad (2.31)$$

$$n_1 + n_2 + n_3 = n \quad (2.32)$$

Solving these equations for  $n_3$  and  $n_2$  gives

$$n_3 = \frac{n_1 C_{13}}{A_{32} + A_{31}} \quad (2.33)$$

$$n_2 = \left[ n_1 C_{12} + \frac{A_{32}}{A_{32} + A_{31}} n_1 C_{13} \right] \frac{1}{A_{21}} \quad (2.34)$$

$$\approx \frac{n_1 C_{12}}{A_{21}} \quad (2.35)$$

Then the ratio of fluxes is

$$\frac{F_{32}}{F_{21}} = \frac{n_3 A_{32} E_{32}}{n_2 A_{21} E_{21}} = \dots = \frac{C_{13}}{C_{12}} \frac{A_{32}}{A_{32} + A_{31}} \frac{E_{32}}{E_{21}} \quad (2.36)$$

Now recalling that the  $C$ 's are related to our  $\alpha$ 's, via, for example,

$$C_{13} = n_3 \left( \frac{2\pi\hbar^4}{km_e^3} \right)^{1/2} \frac{1}{\sqrt{T}} \frac{\Omega_{13}}{g_1} e^{-E_{13}/kT}, \quad (2.37)$$

(2.36) reduces to a function of a bunch of physical constants and the temperature

$$\boxed{\frac{F_{32}}{F_{21}} = \frac{E_{32}}{E_{21}} \frac{A_{32}}{A_{32} + A_{21}} \frac{\Omega_{13}}{\Omega_{12}} e^{-E_{23}/kT}} \quad (2.38)$$

So now given a line strength ratio, we can actually compute a temperature for that diffuse gas. Some examples of ions where these assumptions are valid are  $N^+$ ,  $O^{+2}$ ,  $Ne^{+4}$ , and  $S^{+2}$ .

Now instead if we assume that  $E_{23} \ll E_{12}$  (i.e., the second and third states are very close in energy). This means, though it's not obvious, that  $A_{32} \ll A_{31}$ . Still in the low density limit (ignoring collisional de-excitation), we'll simplify (2.27) and (2.28) again:

$$n_1 C_{13} = n_3 (A_{32} + A_{31}) \quad (2.39)$$

$$\approx n_3 A_{31} \quad (2.40)$$

$$n_1 C_{12} = n_2 A_{21} \quad (2.41)$$

Then the flux ratios are simply

$$\frac{F_{31}}{F_{21}} = \frac{n_1 C_{13}}{A_{31}} \frac{A_{21}}{n_1 C_{12}} \frac{E_{31}}{E_{21}} \frac{A_{31}}{A_{21}} \approx \frac{C_{13}}{C_{12}} \quad (2.42)$$

So the flux rates depend *only* on the collisional excitation rates in this limit. Re-expressing the flux ratio in terms of more fundamental quantities:

$$\frac{F_{31}}{F_{21}} \approx \frac{C_{13}}{C_{12}} \approx \frac{\Omega_{13} e^{-E_{13}/kT}}{\Omega_{12} e^{-E_{12}/kT}} \approx \frac{\Omega_{13}}{\Omega_{12}} \approx \frac{g_3}{g_2} \quad (2.43)$$

for somewhat unobvious reasons. So if we measure line strengths and get this magic number, all we really know is that we're in the low density limit. The magic comes in when we are in the high density limit:

$$\frac{F_{31}}{F_{21}} = \frac{n_3}{n_2} \frac{A_{31}}{A_{21}} \frac{E_{31}}{E_{21}} \quad (2.44)$$

Since in the high density limit there are many collisions, the number densities should be Boltzmann-like:

$$\frac{n_3}{n_2} = \frac{g_3}{g_2} e^{-E_{23}/kT} \approx \frac{g_3}{g_2} \quad (2.45)$$

So the flux ratio is now

$$\frac{F_{31}}{F_{21}} \approx \frac{A_{31}}{A_{21}} \frac{g_3}{g_2} \quad (2.46)$$

So far, this isn't really a density diagnostic, though we've identified the values at both limits. The transition between these limits should be at the critical density discussed earlier, defined by:

$$A_{21}n_2 = n_e n_2 \alpha_{21} \quad (2.47)$$

Earlier, we found that this critical density was found to be

$$n_{e,\text{crit}} = \frac{A_{21}g_2 T^{1/2}}{\beta \Omega_{12}} \quad (2.48)$$

Different transitions will have different critical densities that depend on their intrinsic physics, for electron densities below the smaller critical density, the flux ratio is constant, and the same holds for electron densities greater than the larger critical density. In between, though, there is a transition zone wherein we can approximate a density. Examples of ions that allow for such a diagnostic are  $\text{O}^+$ ,  $\text{S}^+$ ,  $\text{Ne}^{+3}$ , and  $\text{Ar}^{+3}$ .

## 2.3 Energy Level Diagrams

### Suggested References

- Draine Chapter 4

Often we will refer to ions by their atomic name followed by a roman numeral that is one greater than its oxidation state. For instance,  $\text{O}^{+2}$  is referred to as O III. There will be some energy level diagram figures after this demonstrating where some of these energy level assumptions work.

Let's briefly review the electronic configurations of some of these ions. O I has 8 electrons, so in its ground state it has an electronic configuration of  $1s^2 2s^2 2p^4$ . O III however, has a configuration of  $1s^2 2s^2 2p^2$ , where the outermost electrons are actually in different orbitals (remember Hund's rules!). This  $p^2$  configuration disallows the two outermost electrons from having the same quantum numbers ( $n$ ,  $\ell$ ,  $m$ ,  $s$ ). In this case, we know that  $n = 2$  (the "2" in  $2p^2$ ), and  $\ell = \pm 1$  (the  $p$ ). For electrons,  $s = \pm 1/2$ . So the total spin can take on values of 0, or 1 and the total orbital angular momentum can be 0, 1, or 2. We'll often see this configurations labeled via  $^{2S+1}L_J$  where S is the total spin angular momentum, L is the orbital name ( $s$ ,  $p$ ,  $d$ ,  $f$ , etc.), and J is the total angular momentum. The available states for O II are shown in Table 3 Not all of these states are allowed transitions though, for reasons I still need to record here.

$^1D_{J=2}$	$L = 2$	$S = 0$
$^3D_{J=3,2,1}$	$L = 2$	$S = 1$
$^1P_{J=1}$	$L = 1$	$S = 0$
$^3P_{J=2,1,0}$	$L = 1$	$S = 1$
$^1S_{J=0}$	$L = 0$	$S = 0$
$^3S_{J=1}$	$L = 0$	$S = 1$

Table 3: Possible electron configurations for O II.

## 2.4 Infrared Line Diagnostics

Transitions between fine-structure levels of  $p^2$  and  $p^4$  ions are the dominant cooling processes in gas at  $T = 100 - 3000$  K. Examples of such lines are [CII]  $158 \mu\text{m}$  and [OIII]  $88.36 \mu\text{m}$ . Atmospheric water vapor blocks these lines in the 25 to  $300 \mu\text{m}$  range, but airborne observatories can observe them, and ALMA is making great headway in observing mm-scale radiation.

However, note that in the real world (like in H II regions), the ISM is clumpy, so these diagnostics actually only measure the number density of the clumps,  $n_{e,c}$ . The emission measure, however, cares about the average electron density:  $\text{EM} \sim \langle n_e^2 \rangle \times (\text{length})$ . We parameterize this clumpiness with a **volume filling factor** for the clumps,  $f$ , defined by

$$\langle n_e^2 \rangle \approx f n_{e,c}^2 \quad (2.49)$$

Typically we find  $f \sim 0.1 - 0.1$  in nearby H II regions.

## 2.5 Resonance Lines and Selection Rules

Remember that energy transitions are surrounded in square brackets when they are the so-called “forbidden transitions”. The more run-of-the-mill resonance transitions, or allowed transitions, are those that obey the following rules:

1. Only 1 electron involved in the transition
2. Initial and final states have different parity
3. Emitted photon carries 1 unit of angular momentum, so  $\Delta L = \pm 1$
4. Electron spin does not change
5. Change in the total angular momentum of the active electron is  $\Delta J = \pm 1$  or 0, with  $J = 0 \rightarrow 0$  being forbidden.

The statistical weight of any level is  $g = 2J + 1$ .

In addition to the forbidden lines, which break rule 4, there are the intercombination, or **semi-forbidden** lines. These are transitions that break any of the other rules. These transitions are about a million times lower than the resonance transitions ( $A \sim 10^2 - 10^3 \text{ s}^{-1}$  compared to  $\sim 10^8 \text{ s}^{-1}$  for resonance lines). Forbidden lines are several orders of magnitude less prevalent still, as they are

magnetic dipole transitions.

For forbidden or semi-forbidden transitions to be important, we must have very low densities, since higher densities will make collisional processes dominate over these weak transitions. As such, the emitted photons from forbidden transitions are unlikely to be absorbed by another ion, so forbidden line photons usually escape from a nebula and are thus very important coolants. Examples of such transitions are [OIII] 4959, 5007 and [OII] 3726,29

### 2.5.1 Hydrogen Line Series

The line transitions in a de-exciting electron (for instance, a recombination electron that came in at high  $n$ ,  $\ell$  to form an excited hydrogen atom) often produce a series of lines. Transitions that end at  $n = 1$  are called the **Lyman Series**. Transitions from  $n = 2$  to  $n = 1$  are Lyman- $\alpha$  transitions, and those from  $n = 3$  to  $n = 1$  are Lyman- $\beta$  transitions, etc. Similarly, transitions to the  $n = 2$  state form the Balmer series (denoted  $H\alpha$ ,  $H\beta$ , etc.), and the transitions to  $n = 3$  form the Paschen series.

## 3 Molecular Spectra

### Suggested References

- Draine Chapter 5

Molecules present additional complication since rotational and vibrational energies become important. We'll first explore rotating molecules.

### 3.1 Rotating Molecules

Like nearly all forms of atomic energy, the energies of rotating molecules are quantized to energy levels. These rotational energy levels are related to the moments of inertia of the molecules along the various axes of symmetry.

**Example: Linear Diatomic Molecules** Suppose we have a linear diatomic molecule with characteristic lengthscale  $r$  and reduced mass  $\mu$ . Then the moment of inertia of this molecule is

$$I = \mu r^2 \tag{3.1}$$

And the quantized rotational energy levels are

$$E = J(J+1) \frac{h^2}{8\pi^2 I} \tag{3.2}$$

### 3.2 Vibrating Molecules

### 3.3 Molecular Hydrogen

$H_2$  does not radiate strongly because rotational transitions require a heterogeneous linear molecule like CO. In the  $H_2$  molecule, transitions occur via electric quadrupole interaction. The least energetic transition is  $J = 0$  to  $J = 2$ . Thus, lifetimes of excited states are much, much longer than for

the ions (e.g. about 1000 years for the  $J = 2$  level). Hence, the rotational elvels are populated by collisions.

## 4 Transition Rates

We return now to our two-level atom with two states, 1, and 2, separated by an energy gap  $E_{12}$ . We can characterize the rate of decays from state 2 through some characteristic  $e$ -folding time via

$$N_2 = N_2(0)e^{-A_{21}t} \quad (4.1)$$

Here,  $A_{21}$  is proportional to the electric dipole matrix element, or

$$A_{21} \propto e^2 |\langle \psi_1 | \psi_2 \rangle|^2 \quad (4.2)$$

An atom with an electron in state 1 has a probabliity of absorbing a photon given by

$$p_{12} = B_{12}u(\nu_{12}) \quad (4.3)$$

where  $B_{12}$  is the Einstein absorption coefficient and  $u(\nu)$  is the energy density in radiation at a given frequency. We usually derive this energy density from the **specific intensity**,  $I_\nu$  ( $I_\lambda$ ), which has units of energy per area per time per sold angle per frequency (wavelength). The specific intensity is a conserved quantity along a ray of light. To convert this intensity to a flux through some surface, we must integrate this quantity (really, the portion that is normal to the surface) over all incident angles, or

$$F_\nu = \int I_\nu \cos \theta d\Omega \quad (4.4)$$

To get an energy density from the specific intensity (a process we'll discuss later), we use

$$u_\nu = \frac{4\pi}{c} I_\nu \quad (4.5)$$

Similarly, the probability for stimulated emission to occur is

$$p_{21} = B_{21}u(\nu_{12}) \quad (4.6)$$

where the two Einstein coefficients are related via

$$g_1 B_{12} = g_2 B_{21} \quad (4.7)$$

Using LTE, we can derive the spontaneous emission Einstein coefficient to be

## 5 Radiative Transfer

*Wednesday, January 22, 2014*

### 5.1 Basic Definitions

**Energy flux** is the amount of radiative energy that passing through some surface per unit area per unit time. This is in contrast to the **specific intensity**, which is the amount of energy per unit time per unit area per unit solid angle per unit frequency (or sometimes per unit wavelength). Then the total energy through some bundle of rays is given by

$$dE = I_\nu dA dt d\Omega d\nu \quad (5.1)$$

There are several quantities related to the specific intensity

- (0) **Mean Intensity**, defined by

$$J_\nu \equiv \frac{1}{4\pi} \int I_\nu d\Omega \quad (5.2)$$

which is just the specific unit averaged over all solid angles. Note that the differential of solid angle is

$$d\Omega = \sin \theta d\theta d\phi \quad (5.3)$$

This can be thought of as the zeroth moment of the specific intensity.

- (1) Correspondingly, the first moment of the specific intensity is the **specific flux**, given by

$$F_\nu \equiv \int I_\nu \cos \theta d\Omega \quad (5.4)$$

This is essentially the “energy moment” of the specific intensity.

- (2) While the first moment was an energy flux, the second moment is the momentum/pressure moment. Recalling that for a photon,  $p = E/c$ , we can get a momentum flux via

$$P_\nu = \frac{1}{c} \int I_\nu \cos^2 \theta d\Omega \quad (5.5)$$

This is more familiarly known as the **radiation pressure**.

As an example, consider a spaceship some distance  $r$  from a (blackbody) star of radius  $R$  and effective temperature  $T$ . We’d like to know what flux the spaceship observes from the star. Naively we may use the basic equation (5.4) to start:

$$F_\nu = \int B_\nu(T) \cos \theta \sin \theta d\theta d\phi \quad (5.6)$$

$$= B_\nu(T) \int_0^{2\pi} d\phi \int_0^{\theta_{\max}} \cos \theta \sin \theta d\theta \quad (5.7)$$

$$= \pi B_\nu(T) \left( \frac{R}{r} \right)^2 \quad (5.8)$$

where  $\theta_{\max}$  is half the angular diameter of the star as seen from the spaceship,  $\theta_{\max} = \sin^{-1}(R/r)$ .



## 5.2 Equation of Radiative Transfer

Consider a source of radiation shining through some medium to an observer. The change in the specific intensity, in its most general, is given by

$$dI_\nu = -\kappa_\nu I_\nu ds + j_\nu ds \quad (5.9)$$

Where  $j_\nu$  is the **emissivity**, which tells us the rate of emission of radiation of that frequency per unit volume per unit solid angle, or

$$j_\nu \equiv \frac{1}{4\pi} n_u A_{u\ell} h\nu \quad (5.10)$$

In addition to the emissivity, we must also consider the **attenuation**,  $\kappa_\nu$ , which measures the rate at which radiation is absorbed, which is obviously proportional to the incident radiation,  $I_\nu$ . The attenuation has an absorption term and an emission term:

$$\kappa_\nu = n_\ell \sigma_{\ell u}(\nu) - n_u \sigma_{u\ell}(\nu) \quad (5.11)$$

$$= n_\ell \sigma_{\ell u}(\nu) \left[ 1 - \frac{n_u \sigma_{u\ell}}{n_\ell \sigma_{\ell u}} \right] \quad (5.12)$$

$$= n_\ell \sigma_{\ell u}(\nu) \left[ 1 - \frac{n_u/n_\ell}{g_u/g_\ell} \right] \quad (5.13)$$

where in the last step we've used detailed balance to eliminate cross sections in favor of statistical weights. Now in LTE, the number densities of states are given by a Boltzmann distribution:

$$\frac{n_u}{n_\ell} = \frac{g_u}{g_\ell} e^{-h\nu/kT} \quad (5.14)$$

So for sufficiently high frequencies ( $h\nu \gg kT$ ), the second term in (5.13) can be neglected, giving us simply

$$\kappa_\nu \approx n_\ell \sigma_{\ell u} \quad (5.15)$$

This approximation is excellent for the vast majority of astrophysical applications. A notable exception is masers, where stimulated emission is important (note that these are at low wavelengths; microwaves in fact).

### 5.2.1 Example: Lyman Alpha Forest from AGNs

Quasars at  $z \approx 3$  emit strong lyman alpha radiation that travels through a vast expanse of IGM. As it goes through, lyman alpha opacity robs the incident spectrum of lyman alpha radiation. The transition back to the ground state is a permitted transition, so it happens fast and emits photons isotropically. Thus, very few of the absorbed photons are re-emitted in the original direction. Assuming the emissivity vanishes along this path (no spontaneous production of Lyman alpha photons), we get

$$\frac{dI_\nu}{I_\nu} = -\kappa_\nu ds \quad \Rightarrow \quad \ln I_\nu|_s^{\text{obs}} = - \int_s^{\text{obs}} \kappa_\nu ds \quad (5.16)$$

which inspires us to define the **optical depth**, a dimensionless parameter characterizing the relative opacity of a path, via

$$\tau_\nu = \int ds \kappa_\nu \quad (5.17)$$

this gives us another way to express (5.16):

$$I_\nu = I_\nu(s)e^{-\tau_\nu(\text{obs})} \quad (5.18)$$

### 5.2.2 Optical Depth

Thus there are two limiting cases, the optically thin case, where  $\tau \ll 1$  and the optically thick  $\tau \gg 1$  case. A source viewed through an optically thin medium will suffer very little attenuation, whereas a source viewed through an optically thick medium will be almost totally attenuated.

With the optical depth defined, we can recast the equation of radiative transfer neatly in terms of it:

$$dI_\nu + I_\nu d\tau_\nu = \frac{j_\nu}{\kappa_\nu} d\tau_\nu \quad (5.19)$$

to make things work out nicely, we multiply both sides of (5.19) by the integrating factor  $\exp\left(\int_{\text{obs}}^\ell \kappa_\nu ds\right)$  to get

$$\int_s^{\text{obs}} d \left[ e^{\int_{\text{obs}}^\ell \kappa_\nu ds} I_\nu \right] = \int_0^{\tau_\nu} \frac{j_\nu}{\kappa_\nu} e^{\int_{\text{obs}}^\ell \kappa_\nu ds} d\tau \quad (5.20)$$

With some more jiggery-pokery, we get

$$I_\nu(\text{obs}) = I_\nu(s)e^{-\tau_\nu} + \int_0^{\tau_\nu} \frac{j_\nu}{\kappa_\nu} e^{-(\tau_\nu - \tau'_\nu)} d\tau'_\nu \quad (5.21)$$

The first term just give the attenuated original specific intensity, and the second term adds in the sources along the path, each attenuated from its source position to the observer.

Now if the cloud in the medium is in LTE, where the photon emission rate is equal to the photon absorption rate, we have the emissivity of

$$j_\nu \equiv \kappa_\nu B_\nu \quad (5.22)$$

If we are at a uniform temperature,  $T$ , the equation of radiative transfer becomes

$$I_\nu(\text{obs}) = I_\nu(s)e^{-\tau_\nu} + B_\nu(T) \int_0^{\tau_\nu} e^{-(\tau_\nu - \tau'_\nu)} d\tau' \quad (5.23)$$

Now this is an integral we can do, so this simplifies to

$$I_\nu(\text{obs}) = I_\nu(s)e^{-\tau_\nu} + B_\nu(T) (1 - e^{-\tau_\nu}) \quad (5.24)$$

If the very diffuse limit,  $\tau_\nu \ll 1$ , we may take first term expansions of the exponentials to get simply

$$I_\nu(\text{obs}) = I_\nu(s)(1 - \tau_\nu) \quad (5.25)$$

And for the very thick cloud, where  $\tau_\nu \gg 1$ , the exponentials vanish, giving simply

$$I_\nu(\text{obs}) = B_\nu(T) \quad (5.26)$$

### 5.2.3 Radio Astronomy

For radio astronomy, we are typically in the regime where  $h\nu \ll kT$ , so stimulated emission is important. Radio astronomers often speak of a **brightness temperature**, which is the temperature a source would need to have the observed brightness at a particular frequency (this temperature need not be the same for each frequency). Inverting the Planck function, we can get an analytic expression for the brightness temperature:

$$T_B(\nu) = \frac{h\nu}{k} \ln \left[ \frac{2h\nu^3}{c^2 I_\nu} + 1 \right] - 1 \quad (5.27)$$

Radio astronomers will also use an antennae temperature via

$$T_A \equiv \frac{c^2}{2k\nu^2} I_\nu \quad (5.28)$$

The transfer equation becomes

$$\frac{c^2}{2\nu^2 k} I_\nu = \frac{c^2}{2\nu^2 k} I_\nu(s) + \frac{B_\nu c^2}{2\nu^2 k} (1 - e^{-\tau_\nu}) \quad (5.29)$$

or simply

$$T_A(\text{obs}) = T_A(s) + T_c (1 - e^{-\tau_\nu}) \quad (5.30)$$

In the limit where the antennae temperature of the source is much greater than the cloud temperature and the cloud is optically thin, (5.30) simplifies to

$$T_A = T_{A,s}(1 - \tau_\nu) + T_c (1 - (1 - \tau_\nu)) = T_{A,s} - (T_{A,s} - T_c)\tau_\nu \quad (5.31)$$

In the optically thick limit, we just get

$$T_A(\text{obs}) = T_c \quad (5.32)$$

## 5.3 Resonance Line Transfer

**MISSING: MONDAY, JANUARY 27, 2014 (EQUIVALENT WIDTH, CURVE OF GROWTH, ETC.)**

*Wednesday, January 29, 2014*

### 5.3.1 The Voigt Profile

The equivalent width, in wavelength units (though not per unit wavelength), is given by

$$W_\lambda = \frac{\lambda^2}{c} \int (1 - e^{-\tau_\nu} d\nu) \quad (5.33)$$

where the optical depth is

$$\tau_n u = s N \phi(\nu) \quad (5.34)$$

and  $\phi(\nu)$  is the line profile.

From quantum mechanics, we remember that the width of a line is inversely proportional to the lifetime of the state via the uncertainty principle,  $\Delta E \Delta t \sim h$ . This natural shape is the Lorentzian, which is like a sharper Gaussian with stronger wings. In functional form, the natural line profile is then

$$\phi_\nu = \frac{4\gamma_{21}}{16\pi^2(\nu - \nu_{21})^2 + \gamma_{21}^2} \quad (5.35)$$

For a line generated by a transition from state 2 to state 1. To get the width of this line, let's compute the half-width at half maximum (HWHM), or the frequency  $\nu_{\text{HM}}$  where  $\phi(\nu_{\text{HM}}) = 2/\gamma_{21}$ :

$$\frac{4\gamma_{21}}{16\pi^2\Delta\nu^2 + \gamma_{21}^2} = \frac{2}{\gamma_{21}} \quad \Rightarrow \quad \Delta\nu = \frac{\gamma_{21}}{4\pi} \quad (5.36)$$

So the full width at half maximum (FWHM) is

$$\boxed{2\Delta\nu = \frac{\gamma_{21}}{2\pi}} \quad (5.37)$$

For example, for the Hydrogen  $2 \rightarrow 1$  transition, we can look up  $\gamma_{21} = 6.265 \times 10^8 \text{ s}^{-1}$ , which corresponds to a line width or velocity of

$$\Delta v = \frac{\Delta\nu}{\nu_{21}} c = 0.0121 \text{ km s}^{-1} \left[ \frac{\lambda_{21}\gamma_{21}}{7618 \text{ cm s}^{-1}} \right] \quad (5.38)$$

So this is a *very* thin width, especially considering that velocities due to thermal motions are typically much higher than this velocity dispersion. The true line profile then is given by a convolution of the particle velocity distribution and the natural Lorentzian distribution. In general, the velocity distribution of the particles is a Gaussian, and the convolution of a Gaussian and a Lorentzian distribution is called a **Voigt Profile**. Analytically, it looks like

$$\phi_\nu^{\text{Voigt}} = \frac{1}{\sqrt{2\pi}} \int \frac{dv}{\sigma_v} e^{-v^2/(2\sigma^2)} \frac{4\gamma_{21}}{16\pi^2 [\nu - (1 - v/c)\nu_{21}]^2 + \gamma_{21}^2} \quad (5.39)$$

Unfortunately, there is no analytic solution for this integral. Instead, we'll look at two regimes within the Voigt profile.

**Near Line Center (Gaussian)** Near the line center, where the fraction in (5.39) is nearly constant, the profile appears to be a gaussian:

$$s = \sqrt{\pi} \frac{e^2}{m_e c} \frac{f_{12}\lambda_{21}}{b} e^{-v^2/b^2} \quad (5.40)$$

where we've used the **Doppler Parameter**  $b = \sqrt{2}\sigma$ .

**Wings** At large  $\Delta\nu$ , we get

$$s = \sqrt{\pi} \frac{e^2}{m_e c} \frac{f_{12}\lambda_{12}}{b} \left[ \frac{1}{4\pi^{3/2}} \frac{\gamma_{21}\lambda_{21}}{b} \frac{b^2}{v^2} \right] \quad (5.41)$$

**Transition** The transition between these two regimes occurs around

$$e^{z^2} = r\pi^{3/2} \frac{bz^2}{\gamma_{21}\lambda_{21}} \quad (5.42)$$

where  $z \equiv v/b$ . For Ly  $\alpha$ , this corresponds to  $z = 3.2$ , or  $\Delta v = 32 \text{ km s}^{-1}(b/10 \text{ km s}^{-1})$ . Remember that for a Gaussian, the FWHM is  $2\sqrt{2 \ln \sigma}$

Now if the absorbing medium is optically thick at a certain frequency (i.e.,  $\tau_n u > 1$ , then define  $x \equiv v/b$  and again  $v = (\nu - \nu_{21})/\nu_{21}$ ). Define  $x_1$  such that the optical depth is unity at that frequency. The optical depth dies off exponentially as we move away from the resonance frequency,

$$\tau_\nu = \tau_0 e^{-x^2} \quad (5.43)$$

Solving for  $x_1$  then gives us

$$x_1 = \sqrt{\ln \tau_0} \quad (5.44)$$

Taking a Taylor expansion of the attenuation, we find

$$1 - e^{-\tau_\nu} \approx \begin{cases} 1, & \text{for } |x| < x_1 \\ \tau_\nu, & \text{for } |x| \geq x_1 \end{cases} \quad (5.45)$$

Then the equivalent width in units of wavelength is

$$\frac{W(\lambda)}{\lambda_{12}} = 2 \times \frac{\lambda_{12}}{c} \frac{\nu_{12} b}{c} \int_0^\infty (1 - e^{-\tau_\nu}) d\nu \quad (5.46)$$

$$\approx \frac{2b}{c} \left[ \int_0^{x_1} dx + \int_0^\infty \tau_0 e^{-x^2} dx - \int_0^{x_1} \tau_0 e^{-x^2} dx \right] \quad (5.47)$$

$$\approx \frac{2b}{c} \left[ \sqrt{\ln \tau_0} + \tau_0 \frac{\sqrt{\pi}}{2} \left\{ 1 - \text{erf} \left( \sqrt{\ln \tau_0} \right) \right\} \right] \quad (5.48)$$

In the optically thick limit, where  $\tau_0 \rightarrow \infty$ , we may ignore the bracketed term, giving us simply

$$\boxed{\frac{W_\lambda}{\lambda} = \frac{2b}{c} \sqrt{\ln \tau_0}} \quad (5.49)$$

where

$$\tau_0 = \frac{s N_1 \lambda_{12}}{\sqrt{\pi} b} \quad (5.50)$$

Scaling to the Ly  $\alpha$  line,

$$\tau_\nu = 1 \quad \Rightarrow \quad \boxed{N = 8 \times 10^{13} \text{ cm}^{-2} \frac{b}{10 \text{ km s}^{-1}} \frac{1}{f} \frac{1216 \text{ \AA}}{\lambda_{12}}} \quad (5.51)$$

So the “Lyman Alpha Forest” clouds are all optically thin with column densities  $N(\text{H I}) < 10^{14} \text{ cm}^{-2}$ . Then there are Lyman limit systems, which are optically thick. Then finally, there are the Damped Ly  $\alpha$  Absorbers, or DLAs, which we explore now.

For *very* optically thick clouds, where  $\tau_0 > 10^4$ , the attenuation goes as

$$1 - e^{-\tau} \approx \begin{cases} 1, & \text{if } |x| \leq x_1 \\ \tau_0 \frac{a}{\sqrt{\pi}} x^{-2}, & \text{if } |x| > x_1 \end{cases} \quad (5.52)$$

where

$$a = \frac{\gamma_{12}c}{b\nu_{12}} \quad (5.53)$$

Then the equivalent width is

$$\boxed{\frac{W_\lambda}{\lambda} = \frac{2}{c} \sqrt{\gamma_{12}} \lambda_{12}^2 s N_1} \quad (5.54)$$

Again scaling to Ly  $\alpha$ , we get

$$W_\lambda = 7.3 \text{ \AA} \sqrt{\frac{N(\text{HI})}{10^{20} \text{ cm}^{-2}}} \quad (5.55)$$

And now we've identified the three main modes in the curve of growth at small, intermediate, and high column depths.

### 5.3.2 21 cm Line

In the hydrogen atom, the electron-proton spin coupling causes a hyperfine splitting between the two spin states of the electron in neutral hydrogen. The photon emitted through a spin-flip transition has a wavelength of 21 cm. In temperature units, this corresponds to a 0.06816 K. Recalling that the CMB temperature is  $T_{\text{CMB}} = 2.7$  K, the Boltzmann distribution of the two spin states,

$$\frac{n_2}{n_1} = \frac{g_2}{g_1} e^{-h\nu_{12}/kT} \quad (5.56)$$

means that the distribution is largely determined by the statistical weights. Thus,  $n_2/n_1 = 3$  pretty much always. Thus

$$\frac{n_2}{n(\text{HI})} = \frac{3}{4}; \quad \frac{n_1}{n(\text{HI})} = \frac{1}{4} \quad (5.57)$$

The emissivity in the 21-cm line is

$$\gamma_{21} = \frac{n_2 A_{21} h \nu_{21}}{4\pi} \phi(\nu) = \frac{3}{16\pi} n(\text{HI}) A_{21} h \nu_{21} \phi(\nu) \quad (5.58)$$

And the absorption is

$$\kappa_\nu = n_1 \sigma_{12} - n_2 \sigma_{21} \quad (5.59)$$

$$= n_1 \frac{g_2}{g_1} \frac{A_{21}}{8\pi} \lambda_{21}^2 \left[ 1 - e^{-h\nu_{21}/(kT)} \right] \phi(\nu) \quad (5.60)$$

$$\approx \frac{3}{32\pi} A_{21} \frac{hc \lambda_{12}}{kT} n(\text{HI}) \phi(\nu) \quad (5.61)$$

And the optical depth is

$$\tau_\nu = \int_s^o \kappa_\nu ds \quad (5.62)$$

For a Gaussian  $\phi(\nu)$ , we get

$$\tau_\nu = 2.190 \frac{N(\text{HI})}{10^{21} \text{ cm}^{-2}} \left[ \frac{100 \text{ K}}{T} \right] \left[ \frac{\text{km s}^{-1}}{b/\sqrt{2}} \right] e^{-v^2/b^2} \quad (5.63)$$

## 6 Additional Microphysics

### 6.1 Emission and Absorption by a Thermal Plasma

*Monday, February 3, 2014*

Suppose we have a thermal (i.e. Maxwellian) plasma at temperature  $T \sim 8000$  K. The continuum spectrum of such a plasma is *not* simply a blackbody since such a plasma is not necessarily optically thick. Rather, a collection of sources of continuum sources make a rich spectrum. Such sources include recombination (free electrons recombine with ions, giving off an ionization potential plus their kinetic energy into a photon), the two-photon continuum, where an electron undergoes a forbidden transition by giving off two photons that preserve spin properly but whose energies add up to the difference in potential. We'll discuss these processes in more detail now.

**Bound-bound** transitions are those where an electron starts being bound and ends being bound. One such example is cooling via [C II] 158  $\mu\text{m}$ , which is cooling via collisional excitation. The actual volumetric cooling rate is simply given by

$$\frac{\text{energy radiated}}{(\text{time})(\text{volume})} = n_{\text{C}^+} n_{\text{H}} h\nu \alpha_{12} = n_{\text{C}^+} n_{\text{H}} (8.1 \times 10^{-24} \text{ erg s}^{-1} \text{ cm}^{-3}) \quad (6.1)$$

where we can look up the recombination rate,

$$\alpha_{21}(\text{H} - \text{C}^+) = 8 \times 10^{-10} \text{ cm}^3 \text{ s}^{-1} \quad (6.2)$$

and by detailed balance,

$$\alpha_{12} = \alpha_{21} \frac{g_2}{g_1} e^{-92 \text{ K}/T} \quad (6.3)$$

If we assume that hydrogen is mostly neutral and carbon is mostly singly ionized and use typical abundances, we can scale this cooling rate to just the hydrogen number density:

$$\dots = n_{\text{H}}^2 (3.24 \times 10^{-27} \text{ erg s}^{-1} \text{ cm}^{-3}) \quad (6.4)$$

In H I regions, this is a dominant source of cooling.

**Free-Free Emission and Absorption** For free-free radiation, when two charged particles scatter and give off a photon, the power radiated per unit volume scales as

$$P \propto T^{1/2} Z_i^2 n_i n_e \quad (6.5)$$

most of this power is near  $h\nu \sim kT$ . The radio and microwave free-free spectrum is almost flat, declining with increasing frequency as  $\nu^{-0.121}$ . On the absorption side, the attenuation coefficient follows from Kirchhoff's law:  $\kappa_\nu = j_\nu / B_\nu(T)$ . This attenuation is very strong at low frequencies, but negligible in the ISM for  $\nu > 10$  GHz. H II regions can be optically thick at  $\nu < 1$  GHz.

**Bound-free emission**, or radiative recombination, is the process where an ion recaptures an electron, liberating a photon with energy equal to the ionization potential plus the kinetic energy of the electron. The lowest-energy electrons are more likely to be captured by this process, and the rate is thus dependent on the temperature of the gas. In this process, the ion captures the electron,

but the new less-ionized ion is probably still in an excited state. This state will eventually decay to the ground state, emitting one or more photons on the way down. The first photon contributes to the recombination continuum, and the subsequent decays power the recombination lines. Thus, bound-free processes ultimately give rise to strong continuum *and* line emission that depends on the atomic physics of the ion in question.

**Photoionization** is the inverse process of radiative recombination, where a bound electron absorbs a photon and escapes its potential well. For photoionizing an electron, there is a well-known functional form of the photoionization cross section:

$$\sigma(\nu) \approx \sigma_0(Z)\nu^{-3}; \quad \sigma_0(Z) = 6.304 \times 10^{-18} Z^{-2} \text{ cm}^{-2} \quad (6.6)$$

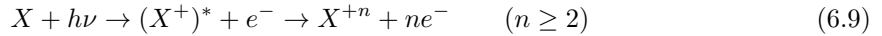
This is only valid for hydrogenic (single electron) ions. It gets more complicated with 3 or more electrons because the resulting ion can be left in a variety of states. The absorption edge is at the minimum photon energy for photon energy for photoionization from a shell. That is, there is a strong edge for hydrogen at  $h\nu = 13.6 \text{ eV}$  below which the cross section vanishes (these photons cannot photoionize the electron). Despite the low abundances present, this can dominate at high energies.

We can relate the cross section for photoionization from a given level to the cross section for recombination to that same level via the Milne Relation. For Hydrogen, we have

$$\sigma = 6.3042 \times 10^{-18} \text{ cm}^2 \left( \frac{\nu}{\nu_0} \right)^{-3.5} \quad (6.7)$$

$$\alpha = 4.18 \times 10^{-13} \left( \frac{T}{10^4 \text{ K}} \right)^{-0.72} \text{ cm}^3 \text{ s}^{-1} \quad (6.8)$$

**X-Ray Fluorescence** is when one electron drops down (from the L shell) to fill the vacancy (K shell), so the atom emits a photon (K $\alpha$ ). Similarly, Auger ionization is when one electron drops down to fill the hole left by X-Ray ionization from the K shell. A second electron is promoted to an excited (and unbound) level. This looks like



Thus, two higher-energy electrons are produced. The inverse of this process is called **di-electronic recombination**. Di-electronic recombination is important in very high-temperature plasmas. When it is important, it often dominates over regular radiative recombination. The electron rarely has enough energy at low temperature to reproduce a doubly excited state. However Mg II and C III are exceptions in which the dielectronic recombination rate is significant at  $10^4 \text{ K}$ . Additionally, this can be important at low temperatures if one of the excited states is a fine-structure state, like C II  $\rightarrow$  C I and others

**Collisional ionization** is very much like the collisional excitation we've talked about before, but enough energy is transferred to fully ionize an electron into the free continuum. There are other processes we haven't covered like three-body processes, charge-exchange, cosmic ray ionization, dissociative recombination, and neutralization by grains.



## 6.2 Collisional Ionization Equilibrium

In a state of collisional ionization equilibrium, the stages of ionization are coupled by the rates for collisional ionization, recombination, and...

All this information can be combined to get a cooling function,  $Q(n_e, T, Z) = \Lambda n_e n$ , which describes the total energy lost by a plasma per unit volume per unit time.

## 7 H II Regions

*Wednesday, February 5, 2014*

### 7.1 Thermal Equilibrium

In a region of gas around a bright star, a pocket of ionized hydrogen can form, driven by the photoionizing radiation from the star. This region is called an **H II Region**. These are usually in thermal equilibrium, where the heating rate is equal to the cooling rate. Heating sources include photoionization from the star, cosmic rays, and collisional de-excitation. The important cooling sources are recombination, free-free processes, and collisional excitation. If the gas is in **ionization equilibrium**, the photoionization and recombination rates are equal as well. That is, the ionization fraction of a given species is constant in time. This means that these two heating/cooling rates are also equal.

The mean energy of a photo-electron is simply

$$\langle E_{\text{pe}} \rangle = \frac{1}{2} m_e \langle v_{\text{pe}}^2 \rangle \quad (7.1)$$

However the mean energy of recombining electrons,

$$\langle E_{\text{recomb}} \rangle = \frac{1}{2} m_e \langle v_{\text{recomb}}^2 \rangle \quad (7.2)$$

is always lower. Thus, these rates being equal actually introduces a net heating process:

$$\Delta E = \frac{1}{2} m_e (\langle v_{\text{pe}}^2 \rangle - \langle v_{\text{recomb}}^2 \rangle) \quad (7.3)$$

This heat source must be balanced by some combination of free-free emission and collisional excitation.

#### 7.1.1 Photoionization Heating

The energy input by photoionization is determined from the stellar spectrum,  $J_\nu$ :

$$\text{Heating Rate} = \int_{\nu_0}^{\infty} \frac{4\pi J_\nu}{h\nu} \sigma_{\text{ph}}(\nu) n_{\text{H}} h(\nu - \nu_0) d\nu \quad (7.4)$$

where  $\nu_0$  is the ionization potential of Hydrogen (13.6 eV/h). The ionization rate is just this without the excess energy term:

$$\text{Ionization Rate} = \int_{\nu_0}^{\infty} \frac{4\pi J_\nu}{h\nu} \sigma_{\text{ph}}(\nu) n_{\text{H}} d\nu \quad (7.5)$$

The average photoelectron energy is just the ratio of these two quantities:

$$\text{Mean Photoelectron Energy} = \frac{\text{Heating Rate}}{\text{Ionization Rate}} \quad (7.6)$$

If we assume a blackbody spectrum,

$$4\pi J_\nu = \pi B_\nu \propto \frac{\nu^3}{e^{h\nu/kT} - 1} \propto \nu^3 e^{-h\nu/kT} \quad (7.7)$$

where we are assuming that the ionization frequencies are on the Rayleigh Jeans tail. The “energy” of the typical photosphere photon is

$$kT_{\text{eff}} = 2.6 \text{ eV} \frac{T_{\text{eff}}}{30\,000 \text{ K}} \quad (7.8)$$

Carrying out all the math (not shown here), we find an approximate form for the average photoelectron energy to be

$$E_{\text{pe}} = \left\langle \frac{3}{2} kT_i \right\rangle \approx kT_{\text{eff}} \left[ 1 - \frac{kT_{\text{eff}}}{h\nu_0} \right] \quad (7.9)$$

This is roughly linear at low temperatures since the second term is negligible. However, when  $kT_{\text{eff}}$  becomes comparable to  $h\nu_0$ , at around 30 000 K, the slope begins to taper off. That is, there is a decreasing return on simply cranking up the temperature of the star.

For an optically thick (at line edge) region, the low energy region of the stellar spectrum (near  $h\nu_0$ ) is effectively removed by the inner regions of the cloud. Thus, at larger distances, there are fewer ionizations (both due to the exponential die-off of higher energy photons in the spectrum and due to the  $\nu^{-3}$  dependence of the ionization cross section). However, those ionizations that do happen are at higher energy, so the mean photo-electron energy is actually higher at larger distances from the source.

### 7.1.2 Cooling By Recombination

The cooling by recombination is given roughly by

$$L_R \propto \frac{1}{2} \langle v_R^2 \rangle n_p n_e \alpha \quad (7.10)$$

where, remember,  $\alpha$  has dimensions of (volume)(time) $^{-1}$ .  $\alpha$  is actually a more complicated term than we might expect:

$$\alpha = \sum_n \sum_L \alpha_{n,L} \quad (7.11)$$

Where the sums are over the transitions from the various energy levels  $n$  and angular momentum states  $L$ . In general,  $\alpha$  scales with the inverse square root of temperature,

$$\alpha \propto T_e^{-1/2} \quad (7.12)$$

and so (due to the thermal energy term in the cooling rate), the cooling rate is proportional to the square root of temperature:

$$L_R \propto \sqrt{T_e} \quad (7.13)$$

Thus hotter gasses cool faster via recombination. A more complete, albeit unclear statement of the cooling rate due to recombination is

$$L_R(H) = n_e n_p k T_e \beta_B(H^0, T) \quad (7.14)$$

where  $\beta$  is now a recombination coefficient that we can look up as a function of the ion in question and the electron temperature. The subscript  $B$  refers to **Case B Recombination**. In fact, the coefficient  $\beta_B$  is more precisely given by

$$\beta_B = \sum_{n=2}^{\infty} \sum_{L=0}^{n-1} \beta_{nL}(H^0, T) \quad (7.15)$$

This means we can ignore all recombinations directly to the ground state (the first sum excludes  $n = 1$ ). The reason we can make this assumption is that in an optically thick cloud, the resulting Lyman continuum photon from a direct recombination will be absorbed so fast so as to effectively cancel out the recombination/ionization event (the mean free path in the standard ISM is less than a parsec). This approximation is known as the **On The Spot** approximation (OTS). If the gas is *not* optically thick, one must use case A recombination approximations.

### 7.1.3 Collisional Cooling

Thus far we have only considered Hydrogen's contribution. However, heavier elements like C, N, O, etc. are important coolants despite their relatively low abundances. Recall that the collisional cross section as a function of relative velocity for a given transition is

$$\sigma_{12}(v) = \frac{\pi \hbar^2}{m^2 v^2} \frac{\Omega(1, 2)}{\omega_1} \quad (7.16)$$

And the cooling rate due to collisional excitation is then (in the low density limit)

$$L_c = n_e n_1 h \nu_{12} q_{12} \quad (7.17)$$

where  $q_{12}$  is ascertained from  $q_{21}$  and detailed balance:

$$q_{21} = \int_0^{\infty} \sigma_{21}(v) f(v) v dv = \frac{8.6 \times 10^{-6}}{\sqrt{T}} \frac{\Omega(1, 2)}{\omega_2} \quad (7.18)$$

And so

$$q_{12} = q_{21} \frac{\omega_2}{\omega_1} e^{-\Delta E/kT} \quad (7.19)$$

In the high density limit,

$$q_{12} n_1 n_e = n_2 A_{21} + n_2 n_e q_{21} \approx \quad (7.20)$$

And so the cooling rate here is given by

$$L_c = n_2 h \nu_{21} A_{21} = n_1 n_e q_{12} h \nu_{12} \left[ \frac{1}{1 + \frac{q_{21} n_e}{A_{21}}} \right] \quad (7.21)$$

From the recombination and collisional cooling rates, we can get a cooling rate. Then by matching the summed cooling rate to our heating rate due to photoionization (and possibly collisional de-excitation), we can identify an equilibrium temperature for the region.

## 7.2 Strömgren Spheres

### 7.2.1 Ionization Equilibrium of a Pure H Nebula

If a pure hydrogen nebula is in ionization equilibrium, the rate of ionizations equals the rate of recombinations:

$$\int_{\nu_0}^{\infty} \frac{4\pi J_{\nu}}{h\nu} \sigma(\nu) n_{\text{H}} d\nu = \alpha(\text{H}, T) n_e n_{\text{H}^+} \quad (7.22)$$

For now we assume that the nebula is large enough that all of the ionizing photons are used in keeping the H II region ionized. What is unclear is whether the edge at which the neutral fraction goes up is sharp or fuzzy. That is, is there a gradual or sharp transition where hydrogen goes from being mostly ionized to mostly neutral?

The mean free path for photons traveling in an H I region is simply

$$\ell \approx \frac{1}{n_{\text{H}^0} \sigma_{\nu_0}} \approx 0.05 \text{ pc} \left( \frac{n_{\text{H}^0}}{1 \text{ cm}^{-3}} \right)^{-1} \quad (7.23)$$

This, compared to the sizes of H II regions, is quite small, so we conclude the transition to neutral hydrogen is rather sharp.

To actually solve for the ionization structure of the nebula, we need to use the equation of radiative transfer:

$$\frac{dI_{\nu}}{ds} = -\sigma n_{\text{H}^0} I_{\nu} + j_{\nu} \quad (7.24)$$

where  $J_{\nu} = 4\pi I_{\nu}$ , and really the radiation field has two components, that from the central star and the diffuse radiation field that arises from recombinations in the [diffuse] nebula:  $J_{\nu} = J_{\nu,*} + J_{\nu,\text{D}}$ . First we'll analyze the field from the star:

$$4\pi J_{\nu,*} = \pi B_{\nu,*} R_* \left( \frac{R_*}{R} \right)^2 e^{-\tau_{\nu}} \quad (7.25)$$

Where the optical depth is

$$\tau_{\nu} = \int_0^R n_{\text{H}^0} \sigma_{\text{ph}} dR \quad (7.26)$$

Now for the diffuse term:

$$4\pi \int_{\nu_0}^{\infty} \frac{j_{\nu}}{h\nu} = n_{\text{H}^+} n_e \alpha_1 = 4\pi \int_{\nu_0}^{\infty} n_{\text{H}^0} \sigma \frac{J_{\nu,\text{D}}}{h\nu} d\nu \quad (7.27)$$

where  $\alpha_1$  is the recombination coefficient that only counts recombinations directly to the ground state, so

$$\alpha_1 \ll \alpha_{\text{A}} = \sum_n \sum_L \alpha_{n,L} \quad (7.28)$$

So the diffuse field is typically much weaker than the stellar radiation field, which allows us to solve for the diffuse field iteratively. Again using our “on the spot” approximation (photons from recombinations to  $n = 1$  are immediately re-absorbed), the diffuse radiation field is

$$J_{\nu,\text{D}} = \frac{j_{\nu}}{n_{\text{H}^0} \sigma} \quad (7.29)$$

and so at ionization equilibrium,

$$4\pi \int \frac{J_{\nu,*}}{h\nu} \sigma n_{\text{H}^0} d\nu + 4\pi \int \frac{J_{\nu,\text{D}}}{h\nu} \sigma n_{\text{H}^0} d\nu = n_{\text{H}^+} n_e \alpha_{\text{A}}(\text{H}, T) \quad (7.30)$$

Simplifying with our approximations, this becomes

$$4\pi \int \frac{J_{\nu,*}}{h\nu} \sigma n_{\text{H}^0} d\nu = n_{\text{H}^+} n_e \alpha_{\text{B}}(\text{H}, T) \quad (7.31)$$

We can now integrate outward from the star to find the ionization fraction, defined by

$$\chi(\text{H}^+) \equiv \frac{n(\text{H}^+)}{n(\text{H}^+) + n(\text{H}^0)} \quad (7.32)$$

Converting (7.31) to variables that know about the star's surface flux, it becomes

$$\boxed{\frac{\pi R_*^2}{R^2} \int \frac{F_{\nu,*}(R_*) e^{-\tau_\nu}}{h\nu} \sigma n_{\text{H}^0} d\nu = n_{\text{H}^+} n_e \alpha_{\text{B}}(\text{H}, T)} \quad (7.33)$$

where the optical depth is, scaled to the optical depth at line edge,

$$\tau = \frac{\sigma(\nu)}{\sigma(\nu_0)} \tau_0(r) \quad (7.34)$$

### 7.2.2 The Strömgren Radius

If we integrate (7.33) outwards and solve for the ionization structure, we get

$$\int_0^{R_{\text{S}}} R_*^2 \int n_{\text{H}^0} \frac{\sigma}{h\nu} \frac{B_{\nu,*}(R_*)}{R^2} e^{-\tau_\nu} 4\pi R^2 d\nu dR = \int_0^{R_{\text{S}}} n_e n_{\text{H}^+} \alpha_{\text{B}}(\text{H}, T) 4\pi R^2 dR \quad (7.35)$$

$$\int_{\nu_0}^{\infty} \pi R_*^2 \frac{B_{\nu,*}(R_*)}{h\nu} \int_0^1 e^{-\tau_\nu} d\tau d\nu = \frac{4\pi}{3} R_{\text{S}}^3 n_e n_{\text{H}^+} \alpha_{\text{B}} \quad (7.36)$$

$$4\pi R_*^2 \int_{\nu_0}^{\infty} \frac{\pi B_{\nu,*}(R_*)}{h\nu} d\nu = \frac{4\pi}{3} n_e n_{\text{H}^+} R_{\text{S}}^3 \alpha_{\text{B}}(\text{H}^0, T) \quad (7.37)$$

Where we've implicitly used the definition of the **Strömgren Radius** as the radius where the optical depth is unity. Physically, we can interpret the left side of (7.37) as the total number of ionizations happening as a result of the stellar radiation field. The right side of (7.37) is just the total number of recombinations occurring within the volume of the Strömgren sphere.

Defining the specific luminosity of the star simply as

$$L_{\nu,*} = 4\pi R_*^2 \pi B_{\nu,*} \quad (7.38)$$

We can define the total number of ionizations more cleanly as

$$Q = N_{\text{ionizations}}(\text{H}^0) \equiv \int_{\nu_0}^{\infty} \frac{L_\nu}{h\nu} d\nu \quad (7.39)$$

Or, in terms of the Strömgren radius,

$$Q = \frac{4\pi}{3} R_S^3 \alpha_B(H^0, T) n_e n_{H^+} \quad (7.40)$$

For a typical density ISM at  $T \sim 10^4$  K,  $Q$  is only dependent on the stellar spectrum. Accordingly, we know that  $Q$ 's for  $O$  stars are significantly bigger than that for, say,  $B$  stars. The same can be said about the corresponding Strömgren radii.

This concept can be extended to galactic scales by summing up the contribution from all massive stars. For a galaxy with a star-forming rate of  $1 M_\odot \text{ yr}^{-1}$ , the galactic  $Q$  value is  $1.08 \times 10^{53} \text{ s}^{-1}$ . We can then calculate the corresponding Strömgren radii for galaxies.

As a more concrete example, consider a blackbody spectrum for our ionizing source. Skipping the integrals, the Strömgren radius is simply

$$R_S \approx 78.2 \text{ pc} \left( \frac{R_*}{R_\odot} \right)^{2/3} \left( \frac{n_{H^0}}{1 \text{ cm}^{-3}} \right)^{2/3} \frac{F_1(x_1)}{x_1} \quad (7.41)$$

Where

$$x \equiv \frac{h\nu}{kT} \quad \text{and} \quad F_1(x_1) = \int_{x_1}^{\infty} \frac{x^2 dx}{e^x - 1} \quad (7.42)$$

where  $x_1$  is  $x(\nu_0)$ .

### 7.2.3 Ionization Parameter

*Wednesday, February 12, 2014*

We should take a moment to define a commonly-used quantity in astrophysics, the **ionization parameter**. Going back to ionization equilibrium, we found the condition for recombinations to balance with photoionization to be

$$\alpha n_e n_p = \int \frac{J_\nu}{h\nu} \sigma n_H d\nu \quad (7.43)$$

Now if we assume that we are in pure hydrogen, we denote the parameter  $\chi$  via

$$n_p = n_e = \chi n_H \quad (7.44)$$

where  $n_H$  is the total number density of hydrogen in any ionization state. Then the number density of neutral hydrogen atoms is simply

$$n_{H^0} = (1 - \chi) n_H \quad (7.45)$$

So now we write the condition for photoionization balance in terms of this new ionization parameter,  $S$ , which will have units of ionizations per unit area per unit time:

$$\alpha \chi^2 n_H^2 \approx \sigma (1 - \chi) n_H S \quad (7.46)$$

Or, moving the ionization fraction  $\chi$  to one side, we get

$$\frac{\chi^2}{1 - \chi} = \frac{S}{n_H} \frac{\sigma}{\alpha} \quad (7.47)$$

We can get some more physical intuition from this formulation, if we note that  $q = S/n_H$  has units of velocity.  $q$  is thus the velocity of the ionization front, if the star were to suddenly “turn on” in the middle of a totally neutral cloud. Often you will see the **dimensionless ionization parameter**, denoted by  $U$ , which is simply

$$U \equiv \frac{q}{c} = \frac{Q}{4\pi R_S^2 n_H c} \quad (7.48)$$

Typical values for  $U$  are in the range of  $10^{-6} - 10^{-1}$ , though it is often used in a steady-state situation.

#### 7.2.4 Effects of Helium

So far we have only considered pure hydrogen, but really we must *at least* consider the impact of helium. If we only care about the region of ionized hydrogen, we’ll need to start caring about which photons ionize helium and which ionize hydrogen. We can still use the “on the spot” approximation for recombinations to the ground state of helium. However, even recombinations to some *excited states* will also be immediately absorbed. The physics is essentially the same, but the accounting is slightly more convoluted. Let’s get into it.

Recall that the first ionization of Helium requires a 24.6 eV photon, and the second ionization potential is 54.4 eV. This second ionization is only relevant for the most massive stars (and bright hot white dwarfs!). Also of importance is the photoionization cross section for helium. At higher energies, helium has a higher cross section than hydrogen, and for the first ionization, the cross section scales as  $\nu^{-2}$  rather than  $\nu^{-3}$ , which is a result of this not being a hydrogenic ion.

So the fate of a 24.6 eV photon depends both on the ratios of the number densities of neutral hydrogen/helium and the ratios of the cross sections. In a cosmic composition, there are about 10 hydrogen atoms for every helium atom, but the relative ionization of hydrogen may be high enough to effectively reduce this ratio. Clearly, the incident spectrum will affect the balance between helium and hydrogen ionizations.

As a result of this competition for 24.6 eV photons the “on the spot” approximation for helium recombination becomes coupled with the hydrogen since it is unclear which type of atom will be ionized by the recombination photon. Schematically, we must have

$$R(\text{H Ionization by Star}) + R(\text{H ionization by He recombination}) + R(\text{H Ionization by He bound-bound}) = R(\text{Rate of H Recombination to } n \geq 2) \quad (7.49)$$

where the various  $R$ ’s are rates. In terms of a more explicit equation, this looks like

$$\frac{R_*^2}{R^2} \int_{\nu_{0,H}}^{\infty} \frac{\pi B_\nu(R_*)}{h\nu} \sigma_{H^0}(\nu) n_H e^{-\tau_\nu} d\nu + y \alpha_{He}(1s) n_{He^+} n_e + p \alpha_B(He) n_{He^+} n_e = \alpha_B n_e n_{H^+} \quad (7.50)$$

where  $y$  is the fraction of photons from helium recombinations to the ground state that ionize hydrogen:

$$y \equiv \frac{\sigma_0(\text{H})n_{\text{H}^0}}{\sigma_0(\text{H})n_{\text{H}^0} + \sigma_0(\text{He})n_{\text{He}^0}} \quad (7.51)$$

and  $p$  is the fraction of helium recombinations that produce bound-bound photons that can ionize hydrogen. The analogous equation for helium is

$$\frac{R_*^2}{R^2} \int_{\nu_0, \text{He}}^{\infty} \frac{\pi B_\nu(R_*)}{h\nu} \sigma_{\text{He}}(\nu) n_{\text{He}^0} e^{-\tau_\nu(\text{He})} d\nu + (1-y)\alpha_{\text{He}}(1s)n_{\text{He}^+}n_e = \alpha_{\text{A}}(\text{He})n_en_{\text{He}^+} \quad (7.52)$$

We should also note that the optical depth changes with distances as

$$\frac{d\tau_\nu}{dR} = \begin{cases} n_{\text{H}\sigma_{\text{H}}}, & \text{if } 13.6 \leq h\nu < 24.6 \text{ eV} \\ n_{\text{H}\sigma_{\text{H}}} + n_{\text{He}\sigma_{\text{He}}}, & \text{if } h\nu \geq 24.6 \text{ eV} \end{cases} \quad (7.53)$$

Thus far we have totally ignored collisional processes. In fact, collisions between helium and protons can cause electrons to jump between excited states, which can move electrons to positions favorable to resonance transitions. So, we should extend this treatment to high- and low-density limits.

In the low density limit, approximately 3/4 of non-ground-state helium recombinations leave the atom in a triplet state, which radiatively decay to the  $2^3\text{S}$  state and subsequently to the  $1^1\text{S}$  state, which radiates a  $\sim 20$  eV photon. About a quarter of these recombinations go to a singlet state, radiatively decaying to the  $1^1\text{S}$  state, which can only decay to the ground state via a two-photon continuum. 56% of the time this process gives one photon energetic enough to ionize hydrogen. Thus in the low density limit,  $p = 0.75 + 0.25(0.66 + 0.33(0.56)) = 0.96$  (since 2/3 of the singlet states are able to decay resonantly and the remaining 1/3 are in the two-photon continuum situation).

In the high density limit, a similar calculation can be done, but many states are collisionally pushed to resonant states, giving  $p = 0.66$ .

As it turns out, the Strömgren radii for helium (first ionization) and hydrogen are roughly equal for high-mass stars ( $T_{\text{eff}} \gtrsim 40,000$  K), and then helium's radius shrinks down to about 20% of hydrogen's for lower-mass stars ( $T_{\text{eff}} \lesssim 30,000$  K). For much more massive stars, there is also a  $\text{He}^{++}$  Strömgren sphere.

MISSING NOTES FROM WEDNESDAY, FEBRUARY 19, 2014 ON RECOMBINATION LINES

## 8 Dust

Friday, February 21, 2014

### 8.1 Evidence for Dust Grains

We see evidence for dust most clearly through its effects on ISM chemistry. Perhaps most importantly is the role dust plays in the formation of molecular hydrogen, as protons latch on to dust



grains and migrate to find each other and form bonds much more efficiently than by direct bonding. We also see that in nearby gas, metal abundances appear lower than solar values, likely because these atoms are locked up in dust grains. Additionally, we indirectly observe dust by its effect on light. It both reflects light and thus polarizes it. In fact, we find a direct correlation between reddening of light and the degree of polarization, indicating that the reddening is caused by dust. In order for light to become linearly polarized, grains must be elongated and aligned. We believe this is due to alignment of grains by galactic magnetic fields.

Dust scatters light very effectively since cross section for such scattering is several orders of magnitude larger than that for Rayleigh scattering by atoms and small molecules. To aid in the description of scattering, we define the **albedo** as the ratio of the scattering cross section to the extinction cross section (reflection vs. absorption). At optical wavelengths, absorption is comparable to scattering, so the albedo is approximately a half. At bluer wavelengths, scattering begins to dominate.

The most nearby example of dust is **zodiacal light**, which is caused by reflection from the sun off of dust grains in the plane of the solar system. This will form the bulk of the background for the James Webb Space Telescope when it comes online.

Dust also plays an important role in reflection nebulae, which scatter UV light from young stars.

We also define the **scattering angle**, which is the average angle of forward scattering when a photon interacts with a dust grain. As it turns out, this scattering isn't isotropic.

## 8.2 Obscuring Effects of Dust

Dust causes extinction, reducing the observed intensity of starlight. This effect can be measured by the Balmer decrement. Earlier we found the expected luminosity of Balmer emission:

$$L(H_\rho) = n_p n_e \alpha_{H_\rho}^{\text{eff}} h \nu_{H_\rho} V \quad (8.1)$$

where  $\rho$  is the actual line being observed ( $\alpha, \beta$ , etc.) and  $V$  is the volume of the cloud. We found that the ratio of these fluxes in case B at  $T \sim 10^4$  K is

$$\left( \frac{F_{H_\alpha}}{F_{H_\beta}} \right)_{\text{emitted}} = 2.86 \quad (8.2)$$

In reality, these fluxes are both attenuated differently by intervening dust:

$$F_{\text{obs}} = F_{\text{em}} e^{-\tau} \quad (8.3)$$

So the observed flux ratio has an attenuation term:

$$\left( \frac{F_{H_\alpha}}{F_{H_\beta}} \right)_{\text{obs}} = \left( \frac{F_{H_\alpha}}{F_{H_\beta}} \right)_{\text{emitted}} \frac{e^{-\tau(H_\alpha)}}{e^{-\tau(H_\beta)}} \quad (8.4)$$

We characterize this extinction with an **extinction curve**,  $f(\lambda)$ , where the optical depth is given by

$$\tau(\lambda) = C f(\lambda) \quad (8.5)$$

Where  $C$  tells us about the cloud's extinction, whereas  $f(\lambda)$  tells us about the radiative transfer details of the line in question. The flux ratio is then

$$\left(\frac{F_{\text{H}\alpha}}{F_{\text{H}\beta}}\right)_{\text{obs}} = 2.86e^{-C(f(\text{H}\alpha)-f(\text{H}\beta))} \quad (8.6)$$

we may look up values for  $f(\lambda)$  for various lines and then solve for  $C$ . In magnitudes, this looks like (calculation omitted):

$$A_\lambda = 1.086\tau_\lambda \quad (8.7)$$

Impressively, the extinction in magnitudes is very close to being the optical depth. Often we'll see extinction written in terms of a **color excess**, defined as

$$E(B - V) = [A(B_1) - A(B_2)] - [A(V_1) - A(V_2)] = \Delta A_B - \Delta A_V \quad (8.8)$$

Essentially this is used to measure the difference in the value of the  $B - V$  color with an "expected" value, quantifying a degree of reddening, or relative extinction. That is, think of comparing to identical stars at identical distances, but one of them is behind a cloud. The obscured one will appear to have a red excess, which we quantify with the color excess. We'll also often see a ratio of the total (or general) extinction to the relative extinction denoted by

$$R_V = \frac{A_V}{E(B - V)} = \frac{E(\infty, V)}{E(B - V)} \quad (8.9)$$

Measuring column depths is impossible for wavelengths shorter than the Lyman limit since the mean free path of such photons is so short due to the prevalence of neutral hydrogen. On the other hand, extremely long wavelength photons are barely extinguished at all. Thus, such diagnostics are relegated to a certain range of wavelengths, the Balmer decrement being an excellent example.

The value of  $R_V$  in galaxies is directly related to the size and shape of dust grains. We find that the wavelength dependence of extinction  $A_\lambda$  in the optical is roughly  $\lambda^{-1}$ , even at 1000 Å. This requires very small grains to make a substantial contribution to the extinction, since  $2\pi a \leq \lambda \Rightarrow a \leq 0.015 \mu\text{m}$ . We see that starlight is significantly polarized at 5500 Å, so the grains with size  $\sim 0.1 \mu\text{m}$  are non-spherical and substantially aligned with the magnetic field. The polarization of starlight decreases towards bluer wavelengths. The grains with  $a \leq 0.05 \mu\text{m}$  which dominate the extinction at  $\lambda < 0.3 \mu\text{m}$  are either spherical or minimally aligned. Most of the mass is in the larger grains, but most of the surface area is in the smaller grains.

There is a peculiar bump in extinction curves at 2175 Å present in the Milky Way, but largely absent in Magellanic Clouds. The best current model for this is a carbon sheet, called the Drude profile. There is also a strong feature in 3.4  $\mu\text{m}$  feature from C-H stretch. Such features can appear as *very* broad lines in spectra, but they are really just properties of the intervening dust.

### 8.3 Thermal Properties of Grains

Dust grains are heated by starlight because non-ionizing photons remove loosely bound electrons from the grain, adding energy to the system. In general, the grain temperature is much less than

the effective temperature of the ionizing source. The heating by photon absorption is roughly given by

$$\left(\frac{dE}{dt}\right)_{\text{abs}} = \int \frac{u_\nu}{h\nu} c h\nu Q_{\text{abs}}(\nu) \pi a^2 d\nu \quad (8.10)$$

and the cooling is a Kirchhoff-like expression:

$$\left(\frac{dE}{dt}\right)_{\text{em}} = \int 4\pi B_\nu(T_{\text{dust}}) C_{\text{abs}}(\nu) d\nu \quad (8.11)$$

Here  $j = \kappa B_\nu(T_{\text{dust}})$